AFOSR-TR- 83-1225

(12)

FINAL REPORT

Reattachment of a Three-Dimensional,
Incompressible Jet to an Adjacent
Axisymmetric Inclined Surface

March 31, 1983

Principal Investigator:

Eugene E. Niemi, Jr.
University of Lowell
Lowell, Massachusetts 01854

83 12 27 16

REPORT DOCUMENTATION PAGE	READ INSTRUCTIONS BEFORE COMPLETING FORM

1. REPORT NUMBER AFOSR-TR- 83-1225	2. GOVT ACCESSION NO.	3. RECIPIENT'S CATALOG NUMBER

4. TITLE (and Subtitle)	5. TYPE OF REPORT & PERIOD COVERED
REATTACHMENT OF A THREE-DIMENSIONAL, INCOMPRESSIBLE JET TO AN ADJACENT AXISYMMETRIC INCLINED SURFACE	FINAL 15 Apr 82 – 31 Jan 83
	6. PERFORMING ORG. REPORT NUMBER

7. AUTHOR(s)	8. CONTRACT OR GRANT NUMBER(s)
EUGENE E NIEMI JR	AFOSR-82-0215

9. PERFORMING ORGANIZATION NAME AND ADDRESS	10. PROGRAM ELEMENT, PROJECT, TASK AREA & WORK UNIT NUMBERS
UNIVERSITY OF LOWELL RESEARCH FOUNDATION 450 AIKEN STREET LOWELL, MA 01854	61102F 2307/D9

11. CONTROLLING OFFICE NAME AND ADDRESS	12. REPORT DATE
AIR FORCE OFFICE OF SCIENTIFIC RESEARCH/NA BOLLING AFB, DC 20332	March 1983
	13. NUMBER OF PAGES 44

14. MONITORING AGENCY NAME & ADDRESS(if different from Controlling Office)	15. SECURITY CLASS. (of this report)
	UNCLASSIFIED
	15a. DECLASSIFICATION/DOWNGRADING SCHEDULE

16. DISTRIBUTION STATEMENT (of this Report)

Approved for Public Release; Distribution Unlimited.

17. DISTRIBUTION STATEMENT (of the abstract entered in Block 20, if different from Report)

18. SUPPLEMENTARY NOTES

19. KEY WORDS (Continue on reverse side if necessary and identify by block number)
THRUST REVERSER
COANDA EFFECT
REATTACHMENT
THREE-DIMENSIONAL FLOW

20. ABSTRACT (Continue on reverse side if necessary and identify by block number)
A study has been made of the fluid mechanics of a thrust reverser jet reattaching to an aircraft nozzle afterbody. The problem basically involves the Coanda effect flow of a three-dimensional, incompressible jet to an adjacent axisymmetric, inclined surface. The equations have been derived in integral form and programmed for numerical solution for the case of an exhaust flow with no opposing free stream flow. Test data are reported for a scale model of a nozzle afterbody exhausting against a target-type thrust reverser. Data are presented for surface pressure coefficient at various

DD FORM 1473 EDITION OF 1 NOV 65 IS OBSOLETE
1 JAN 73

points along the model. Recommendations are made for future research in this area.

Abstract

A study was been made of the fluid mechanics of a thrust reverser jet reattaching to an aircraft nozzle afterbody. The problem basically involves the Coanda effect flow of a three-dimensional, incompressible jet to an adjacent axisymmetric, inclined surface.

The equations were derived in integral form and programmed for numerical solution for the case of an exhaust flow with no opposing free stream flow.

Test data are reported for a scale model of a nozzle afterbody exhausting against a target-type thrust reverser. Data are presented for surface pressure coefficient at various points along the model.

Recommendations are made for future research in this area.

A

Table of Contents

I. Introduction and Background

The U.S. Air Force has shown recent interest in the use of thrust reversers on future models of fighter aircraft. Thrust reversers are being considered for use both as a tactical maneuvering device in the transonic speed range, as well as for more conventional use during the landing mode.

A number of problems can arise when thrust reversers are used on aircraft. One particular problem that can occur when thrust reversers are deployed in flight is the attachment of the reversed jet to the aircraft afterbody and fuselage. This phenomenon has been reported in wind tunnel tests of full size aircraft in references 1 and 2, and for model scale wind tunnel tests in reference 3.

The current research is for the purpose of developing a theoretical method for predicting conditions under which a reversed exhaust jet will attach to an aircraft afterbody. The original proposal for this research is reference 4.

II. Literature Survey

The thrust reverser flow attachment is basically a variation of the Coanda effect. The Coanda effect finds one of its more useful applications in the field of fluidics. Therefore, some of the work reviewed is related to fluidics.

One of the earliest analyses of Coanda effect that was studied in detail was the work of Bourque and Newman[5]. Bourque and Newman developed a simplified theory for predicting jet attachment distance for a two-dimensional, incompressible jet exiting near an adjacent flat plate. In this study, the surrounding fluid was at rest.

Experimental data were also reported and compared with the theory. The agreement was generally fair to good.

Bourque and Newman described the jet attachment hysteresis effect in terms of the range of angles over which an incompressible jet would attach to an adjacent sidewall. It was found that the flow could be attached or detached depending on how the flow was initiated.

Perry[6] developed a theory for predicting reattachment location for an incompressible jet by making several improvements to the theory of reference 5. Perry compared his theory with his own experimental data as well as the experimental data of reference 5, and it was shown that some improvement was obtained in the agreement 'between theory and experiment.

Olson[7] extended the above studies to two dimensional, compressible flow, and compared the theory to test data. Olson's theory involved a trial and error numerical procedure. Two values of constants that appear in the theory had to be evaluated from experimental data. The theory was developed to handle both setback and slope of side walls.

In reference 8, an experimental study was made of the effect of jet Reynolds number on location of attachment point. It was found that a hysteresis effect occurred for flow attachment in terms of an upper and lower Reynolds number. Experiments and flow visualization were done for low speed water flows. The experiments were done for a three-dimensional, rectangular exit nozzle geometry roughly approximating two-dimensional conditions. No theory was developed in this reference.

The most recent work located on this topic was that of Hoch and JiJi[9]. They extend the theory of references 5 and 6 and develop a theoretical model to predict incompressible jet reattachment in the presence of a parallel free stream. More realistic assumptions are made for pressure, velocity, and jet radius of curvature in the preattachment region. The model uses boundary layer type velocity profiles and a semi-empirical pressure spread coefficient determined from comparisons with experimental data. Good correlation is obtained between theory and experimental data.

A study of a thrust reverser's effect on the exhaust jet flow field was performed by Sarpkaya and Hiriart[10]. A detailed study was made of the effect of various thrust reverser shapes on the shape and orientation of the flow leaving the reverser. However, no work was done on subsequent reattachment of the jet to the aircraft afterbody.

It is seen that no work appears to have been done on the problem of the reattachment of an axisymmetric jet to an aircraft afterbody.

III. Development of Theory

A number of possible theoretical approaches are possible -- the one to be taken based on time and funds available for the conduct of the project. Various potential flow and perfect fluid theories are available, a number of these available in computer code form, such as finite difference and finite element analyses. These might be useful in determining the pressure and velocity field in the neighborhood of the jet, but cannot be used to determine the j t behavior itself (such as attachment conditions), because the attachment effect is a viscous entrainment phenomenon.

Ordinary viscous flow theories, such as boundary layer programs, will probably not be directly useful either, since they do not allow for the type of fluid entrainment and flow against a primary main stream that is occurring in this problem.

Considerable time was spent reviewing different theoretical approaches that might be applied to the problem, including the advanced methods presented in references 11 and 12. Based on this review, it was decided that the time and funds available would have to limit the study to the development of a basic theory to predict the essential characteristics of the flow being studied. As will be seen in later sections, some of the inputs to the theory required obtaining some experimental data, and a slight shift in the emphasis originally proposed.

Assumptions and Equations

The approach used for this investigation is illustrated in Figure 1. The flow from the nozzle afterbody exits rearward in the +Z
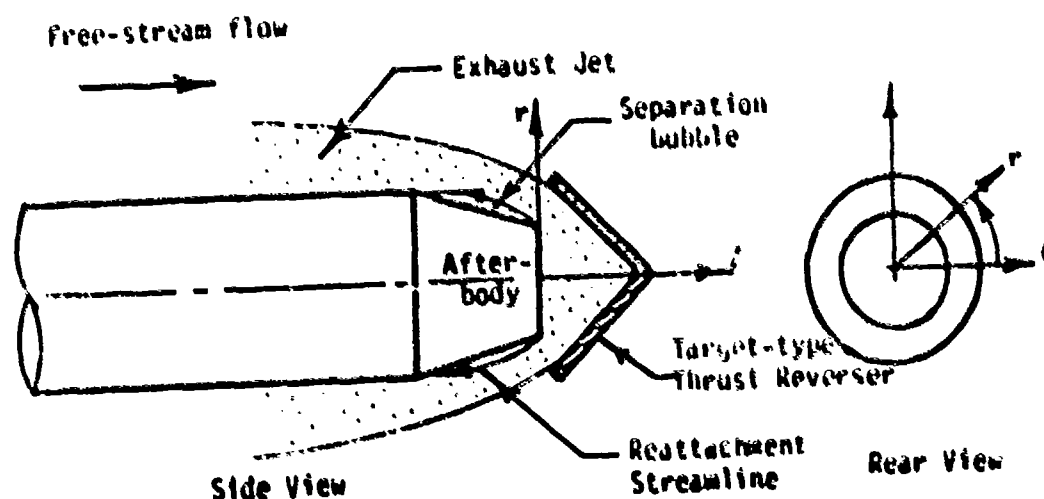
Figure 1. Flow Geometry for Reattached Jet

direction until it hits the target-type thrust reverser, whereupon the
flow is turned forward in a direction generally parallel to the
sloping afterbody sides. For the case of flow reattachment, a
separation bubble is formed between the jet exit and the point where
the flow finally reattaches to the afterbody. The geometry of the
nozzle/afterbody was chosen similar to one of those investigated
experimentally for other effects in reference 13.

The assumptions that have been made to develop the theory are as
follows:

1)   Steady, incompressible flow.

2)   Three dimensional, axisymmetric flow.

3)   Exhaust flow is Newtonian fluid.

4)   Negligible diffusion between flows.

5)   Entrainment of fluid similar to that of a free jet.

This leads to an integral approach to the problem, with simplified
models for the entrainment effects and pressure and velocity profiles.

The geometry used for derivation of the equations for the flow
field is shown in Figure 2.

The derivation generally follows the approach presented in
reference 7, but with modifications as necessary to account for
differences in geometry. Semi-empirical factors for the theory might
also be different and have to be obtained from experiments. All
symbols are defined in the numenclature section of this report.
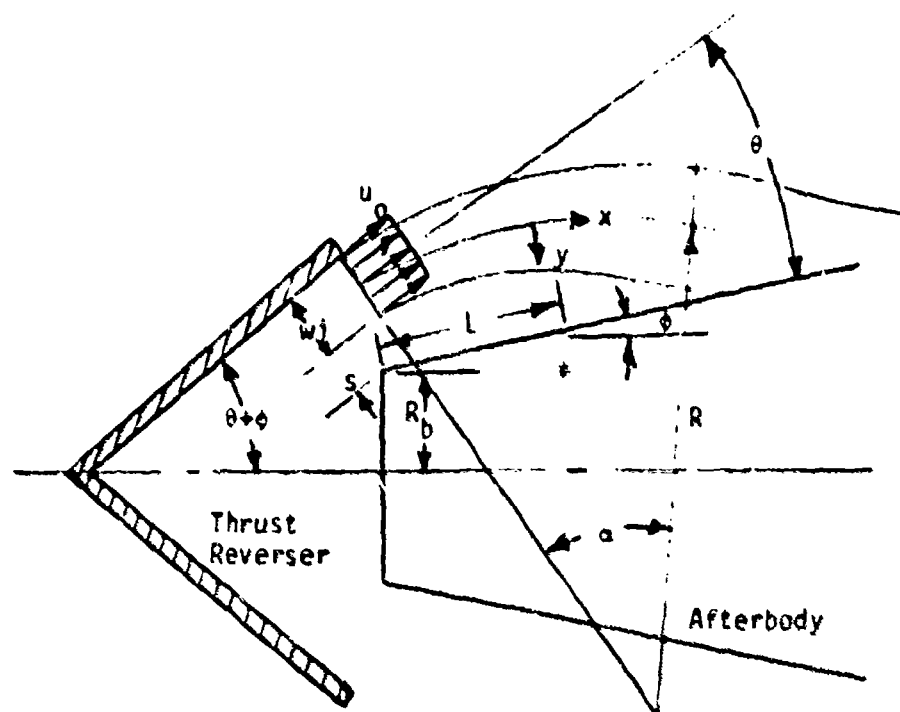
Figure 2. Flow Field Near Reattachment

The radius of curvature of the exhaust jet is given by

$$R = \left[\frac{(\rho u_0^2/p_0) \, Rj \, wj}{1 - p_i/p_0} \right]^{1/2} \tag{1}$$

The non-dimensional distance between the jet centerline and the boundary wall, Δ/wj is given by

$$\frac{\Delta}{wj} = \frac{R}{wj} - \left\{ \left(\frac{L}{wj} \cos \theta \right)^2 + \left[\frac{R}{wj} - \left(\frac{1}{2} + \frac{S}{wj} + \frac{L}{wj} \sin \theta \right) \right]^2 \right\}^{1/2} \tag{2}$$

The non-dimensional distance along the jet centerline is given by

$$\frac{x}{wj} = \frac{R}{wj} \, \alpha \tag{3}$$

6

where the angle α is given by

$$\alpha = \tan^{-1} \left[\frac{\frac{L}{wj} \cos \theta}{\frac{R}{wj} - (\frac{L}{wj} \sin \theta + \frac{S}{wj} + \frac{1}{2})} \right] \qquad (4)$$

The velocity distribution in the jet is assumed to satisfy the equation[5]

$$u = \left[\frac{3 J \alpha}{4\rho(x + x_0)} \right]^{1/2} \text{sech}^2 \frac{\sigma y}{x + x_0} \qquad (5$$

The position of the separation streamline, δ/wj, is obtained by numerically integrating the mass flow in the jet from the centerline for small increases in y/wj, assuming the jet characteristics upstream of reattachment are given by (5). The integration is continued until the mass flow equals one-half the mass flow in the jet at the point where it leaves the thrust reverser. The resulting value of y/wj is taken as the position of the separation streamline.

With δ/wj known, equations (1) through (4) can be used to calculate the reattachment location as a function of the mean pressure in the separation bubble using the condition that $\Delta/wj = \delta/wj$ at reattachment.

The mean pressure in the separation bubble, divided by the pressure on the free boundary of the jet becomes

$$\frac{p_i}{p_e} = 1 + (\frac{I_0 + I_1}{Ap_0}) \cos \alpha - K_2 (\frac{p_s}{p_0} - 1) \frac{A' \cos \alpha}{A} - \frac{\rho_0 U_0^2}{p_0} (\frac{2\pi R jwj}{A}, \qquad (6)$$

In this equation, I_0 is the momentum of all the flow in the downstream direction at x'/wj, and I_1 is the momentum of the downstream flow at x'/wj that is reversed back into the separation bubble at reattachment. The stagnation pressure on the separation streamline is given by p_s, and K_2 is an empirical constant related to the fraction of

7

pressure force effective in reversing the flow momentum at reattachment.

The area expressions in equation (6) are given in equations (7) and (8):

$$A = 2\pi R' (s + L' \sin \theta) + \pi (s + L' \sin \theta)^2 \cos (\theta + \phi) \qquad (7)$$

$$A' = 2\pi R' (\Delta' - \delta') + \pi (\Delta' - \delta')^2 \cos [\alpha - (\theta + \phi)] \qquad (8)$$

In equation (7), L' is the value of L to the point in the jet where the static pressure can be assumed constant across the jet and equal to the static pressure on the outer boundary of the jet. The location of this downstream boundary at x'/w_j is taken as some fraction K_1 of the value of x/w_j at reattachment. The value of K_1 must be determined empirically.

Solution of Equations

Equations (1) through (8) can be solved by an iteration technique similar to that proposed in reference (7) to determine the jet reattachment location for the case where there is a reattaching exhaust jet flow but no opposing free stream flow. The equations also give the jet trajectory in the preattachment region, the axial velocity decay in the jet, and the wall pressure in the separation bubble. The case of free stream flow is discussed in Section VI.

In order to solve these equations, however, two empirical constants, K_1 and K_2 are needed, as well as use of an empirical jet spread equation. Evaluation of the existing literature has revealed no available jet spread equation for axisymmetric flow that can be

8

used as a more accurate replacement for equation (5). This equation predicts the effects of both jet spread and entrainment for a two dimensional jet.

To validate any solutions from the theory outlined above, some experimental data will eventually be needed. Thus, it became apparent that some change in the emphasis of the original research proposal would be necessary, a change from a completely theoretical study to a theoretical study supplemented by experiments. As a result, a parallel experimental study was undertaken and is described in the next section. Some results of the theory are discussed in Section V.

IV. Experimental Work

Figure 3 is an illustration of a model that has been constructed to study flow reattachment in three-dimensional axisymmetric flow. The nozzle-afterbody section of the model is similar in design to one used in tests reported in reference 13.
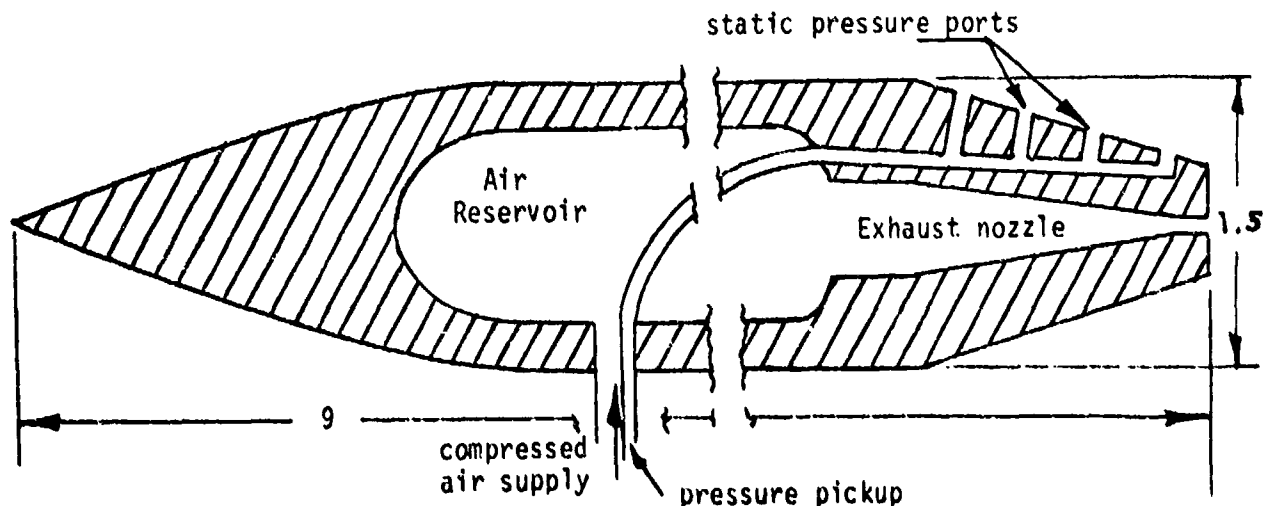
Figure 3. Schematic of Model Used for Experiments

The model is provided with compressed air which discharges through a conventional aft-mounted nozzle. Not shown in the figure is a target-type thrust reverser which causes the exhaust to flow forward along the afterbody. Four static pressure orifices located along the afterbody were used to measure pressures.

Figures 4a and 4b are photographs of the model and its mounting for the University of Lowell low speed wind tunnel. Tests were conducted at several free-stream velocities and nozzle pressure ratios, and at various thrust reverser set-back distances. Two sizes of nozzle throat opening were tested.

A matrix of the more important conditions tested is given in Table 1. Tests were made at other conditions also, but are not reported in this study.
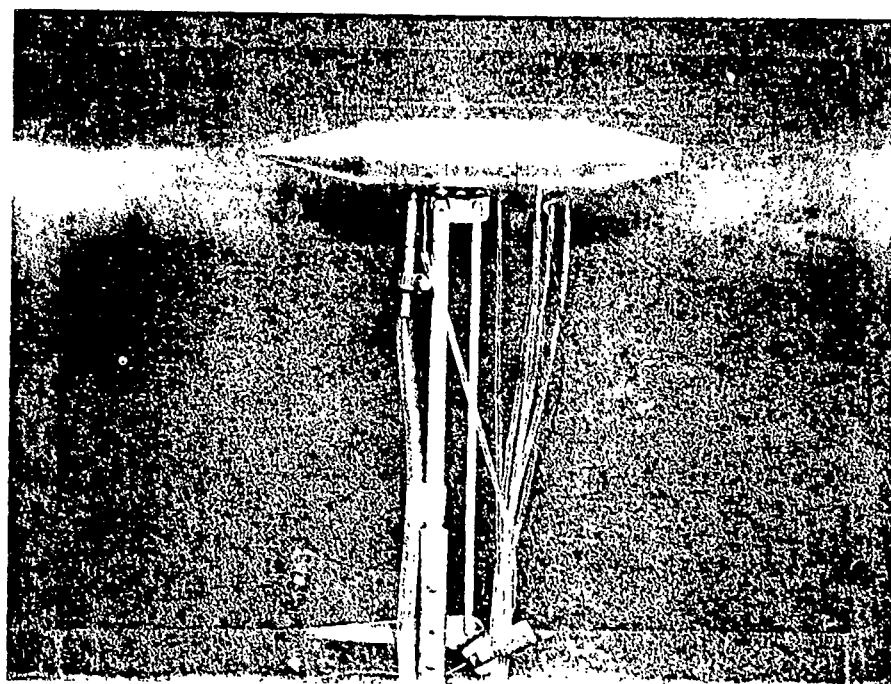
Figure 4a. Model Showing Pressure Pickups
and Compressed Air Line
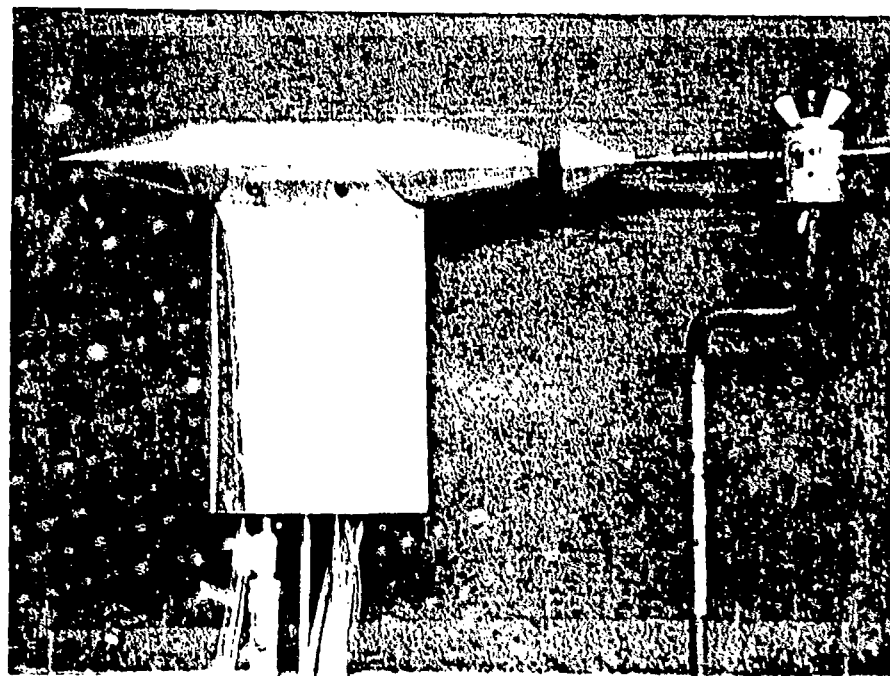
Figure 4b. Model with Fairing over Lines
and Thrust Reverser Mounted

11

Table 1

Test Condition Matrix

Test Nos.	Thrust Reverser Configuration	Distance reverser mounted aft of nozzle exit (inches)	Nozzle stagnation pressure (psig)	Free-stream velocities* (fps)
1-3	Not installed	-	0	51.3, 58.7, 70.4
4-6	↓	-	30	
7-9	Installed	0.125	0	
10-12			10	
13-15			15	
16-18			20	
19-21			25	
22-24			30	
25-27	Installed	0.250	0	
28-30			10	
31-33			15	
34-36			20	
37-39			25	
40-42	↓	↓	30	↓

*Note: Tests were also run at zero free-stream velocity.

Test Results

Static pressures were measured at four locations on the afterbody and at several forward stations as well. These pressures were converted into pressure coefficients. Plots of pressure coefficient versus body location are presented in Appendix B.

The test data are discussed in Section V.

V. Solution of Flow Equations

Time and funds available did not allow completion of the solution of the equations or a complete interpretation of the test data. However a representative test case for no free stream flow was chosen and programmed for solution on the computer. The input data for this case are summarized in Table 2 below.

Table 2

Flow Input Conditions

Geometry:

Afterbody surface slope, ϕ	15°
Angle between initial jet direction and afterbody, θ	30°
Base radius of afterbody, R_b	0.277 in.
Initial width of jet, w_j	0.0021 in.
Jet setback distance, s	0.175 in.

Flow Conditions:

Jet density, ρ	0.00444 sl/ft^3
Initial jet velocity, u_0	1031 fps
Free stream pressure, p_0	2101 psfa
Jet spread parameter, σ	7.7

The equations were programmed in Fortran IV for solution on the University of Lowell Computer System, using a program called ATTACH.

Appendix A contains a printout of the program statements and output, for one particular case corresponding to experimental data.

A plot of the jet trajectory and spread rate for a wall pressure of p_j = 2099 psfa is shown in Figure 5. These plots are from the

13
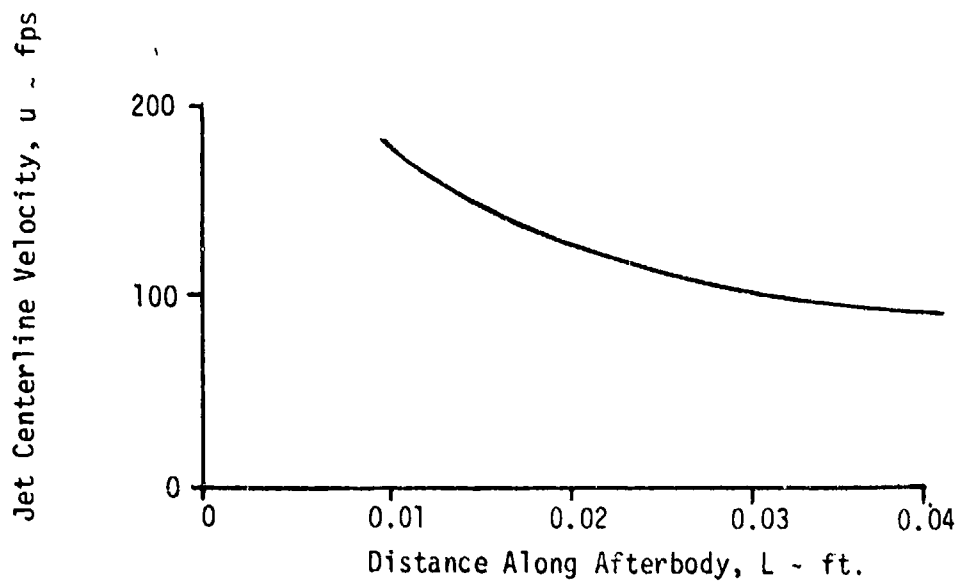
Figure 5a. Variation of Jet Centerline Velocity
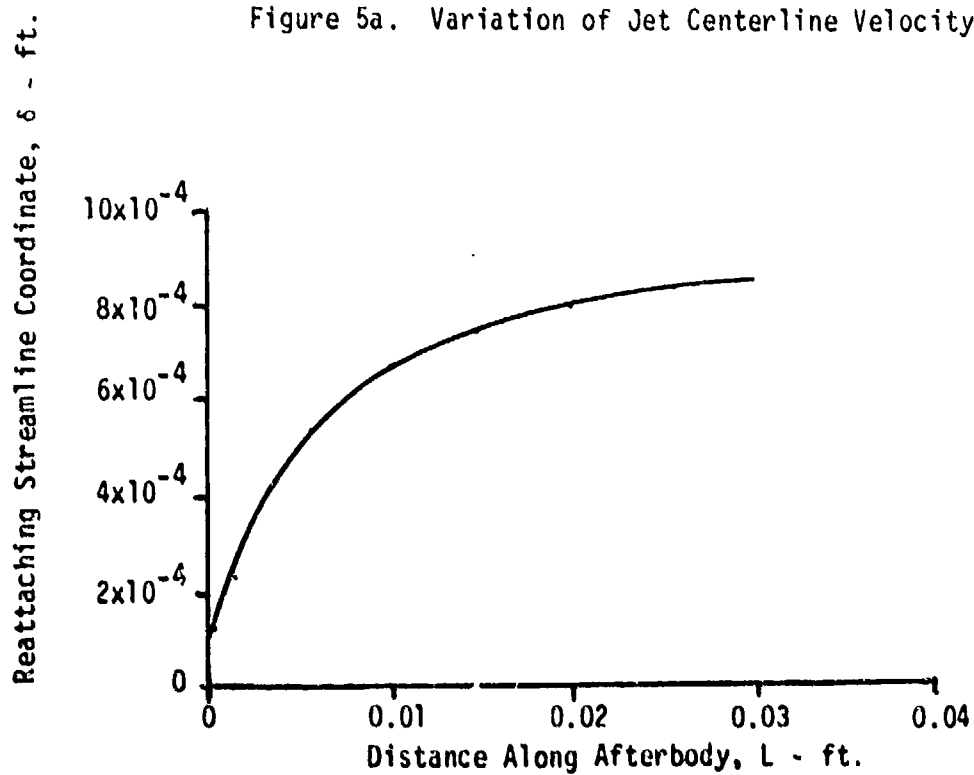
Figure 5b. Jet Spread Variation

14

computer output of Appendix A. The available time and funds for this research project did not allow the comparison of these calculations with the test data shown in Appendix B.

VI. Recommendations for Future Work

The following recommendations are made for additional work in this area:

1) Completion of programming the equations and verification of their validity for certain flow conditions.

2) Extension of the development and solution of the equations to the case of an opposing free stream flow.

The following experimental work is needed to verify some of the assumptions used in the theory:

3) Flow visualization at low Reynolds numbers by using the existing model in a water channel and photographing the extent of the reversed flow in an opposing free stream. This would be done by using a colored fluid in the exhaust flow to contrast with clear water in the main stream flow.

4) Similar visualization of the flow at somewhat higher Reynolds numbers in the low speed wind tunnel using smoke or steam for the exhaust flow and air for the opposing flow.

The experiments described in items 3 and 4 will provide important information on attachment, the extent of reversed flow against the main stream, and verification of the selection of suitable values for the constants K_1 and K_2 and the jet spread equation.

VII. Conclusions

The equations have been derived for the case of attached flow
from a thrust reverser impinging on a nozzle-afterbody. These
equations were derived for the case of no opposing free stream flow.
The portion of these equations for the jet spread and jet trajectory
have been programmed in Fortran IV and solved on a computer.

Experiments have been conducted on a small scale model with a
target type thrust reverser, and measurements have been made of
surface pressure distribution for various combinations of nozzle flow
and free stream velocity.

Recommendations have been made for future work. These include
additional experiments in flow visualization to aid in determining
empirical constants required in the theory, and an extension of the
theory to the case of an opposing free-stream flow.

References

1. Tolhurst, W.H., Jr., Kelly, M.W., and Greif, R.K., "Full-Scale Wind Tunnel Investigation of the Effects of a Target-Type Thrust Reverser on the Low-Speed Aerodynamic Characteristics of a Single Engine Jet Airplane," NASA TN D-72, Sept., 1959.

2. Falarski, M.D., and Mort, K.W., "Full-Scale Wind Tunnel Investigation of a Target-Type Thrust Reverser on the A-37B Airplane," NASA TM X-1985, Ames Research Center, April, 1970.

3. Munnicksma, R., "Some Experience with Jet Reverser Model Testing, using Hot and Cold Jets in Ground Proximity," Proc. of the 35th Semi-Annual Meeting of the Supersonic Tunnel Association, Vought Aeronautics Co., Dallas, Texas, March 8-9, 1971.

4. University of Lowell Proposal No.: 82-76, "Reattachment of a Three-Dimensional, Incompressible Jet to an Adjacent Axisymmetric Inclined Surface," University of Lowell Research Foundation, Lowell, MA, 26 October 1981.

5. Bourque, C., and Newman, B.G., "Reattachment of a Two-Dimensional, Incompressible Jet to an Adjacent Flat Plate," The Aeronautical Quarterly, Vol. XI, Aug., 1960.

6. Perry, C.C., "Two-Dimensional Jet Attachment," Ph.D. Dissertation, Mechanical Engineering, University of Michigan, 1967.

7. Olson, R.E., "Reattachment of a Two-Dimensional Compressible Jet to an Adjacent Plate," Presented at the Symposium on Fluid Jet Control Devices, Winter Annual Meeting of ASME, New York, Nov. 28, 1962.

8. Comparin, Glaettli, Mitchell, and Mueller, "On the Limitations and Special Effects in Fluid Jet Amplifiers," Presented at the Symposium on Fluid Jet Control Devices, Winter Annual Meeting of ASME, New York, Nov. 28, 1962.

9. Hoch, J., and Jiji, L.M., "Two-Dimensional Turbulent Offset Jet Boundary Interaction," Journal of Fluids Engineering, Vol. 103, March, 1981.

10. Sarpkaya, T., and Hiriart, G., "Analysis of Curved Target-Type Thrust Reversers," Journal of the American Institute of Aeronautics and Astronautics, Vol. 13, No. 2, February 1975.

11. Whitfield, D.L., "Integral Solution of Compressible Turbulent Boundary Layers Using Improved Velocity Profiles," AEDC-TR-78-42, Arnold Engineering Development Center, Tenn., Dec., 1978.

12. Jacocks, J.L., and Kneile, K.R., "Computation of Three-Dimensional Time-Dependent Flow Using the Ewler Equations," AEDC-TR-80-49, Arnold Engineering Development Center, Tenn., July, 1981.

13. Robinson, C.E., "Evaluation of Reynolds Number and Tunnel Wall Porosity Effects on Nozzle Afterbody Drag at Transonic Mach Numbers," AEDC-TR-76-70, July, 1976.

Nomenclature

Symbol	Definition
A	Term expressing area function in control volume
α	Angle to particular location in jet
α'	Value of α at reattachment
A'	Term expressing area function in control volume
C_p	Surface pressure coefficient, $p-p_0/\frac{1}{2}\rho V_0^2$
Δ	Distance from surface to jet centerline
Δ'	Value of Δ at reattachment point
δ	Value of y at reattachment streamline border
δ'	Distance from jet center to reattaching streamline
K_1	Fraction of distance in momentum equation
K_2	Fractional portion of pressure difference (p_s-p_0) effective in returning flow
L	Distance along surface of afterbody
L'	Surface distance to point where surface pressure equals jet pressure
p	Local surface pressure
p_e	Pressure external to jet $(p_e=p_0)$
p_i	Pressure inside separation bubble
p_{in}	Nozzle stagnation pressure
ϕ	Afterbody surface slope
p_0	Jet and external pressure
p_s	Stagnation pressure on reattaching streamline
R_s	Radius of center streamline of jet
R_b	Base radius of afterbody
ρ	Density of tunnel flow
ρ_0	Density of jet
R_j	Radius to annular jet from reverser
R^J	Afterbody radius to point where $L=L'$
S	Jet setback distance
σ	Jet spread parameter
θ	Angle between initial jet direction and afterbody surface
u	Velocity at any general position in jet
u_0	Initial jet velocity
V_0	Tunnel test section velocity
w_j	Width or thickness of annular jet
x	Distance along curved center streamline
y	Coordinate perpendicular to center streamline
I_0 or J	Initial momentum of jet
I_1	Fraction of forward momentum entrained
I_2	Momentum of return flow from jet
J^2	Momentum of jet at nozzle exit
x_0	Distance measured back to theoretical jet exit, or thrust reverser setback
x'	Value of x at reattachment location

APPENDIX A

Computer Program Printouts

```
      PROGRAM WITCH(INPUT,OUTPUT,TAPE5=INPUT,TAPE6=OUTPUT)
      DIMENSION X(50),AL(50),BE(50)
      DIMENSION X(50),Y(50),U(30,50),UFLO(30,50),FLOW(30,50)
      DIMENSION DELT(50)
      REAL L(20)
      PHI = 15./57.296
      TH = 30./57.296
      AJ = 0.00171
      SIG = 7.7
      UU = 1031.
      RHO = .00049
      RJ = .0499
      S = .1455
      XU = .0003755
      PU = 2100.
      PI = 2090.
      UY = U/10.
      B = 0.0230
      XL = .0
      XY = .0
      XU = .0
      AIU = 5.283*RHO*UU*RJ*(UU**2.)
      EXFL = .50000*RJ*UU
      WRITE(10,350) EXFL
 350  FORMAT(5X,F10.6)
      R = ((RHO*RJ*AJ*UU**2.)/(PU-PI))**.50
      DO 540 I = 1,20
      L(I)=L(I-1)+.01
      FL=RO+L(I)*SIN(PHI)
      DEL(I) = R-SQRT((L(I)*COS(TH))**2.+(R-.5+RJ-S-L(I)*SIN(TH))**2.)
      AL(I) = ATAN((L(I)*COS(TH))/(R-L(I)*SIN(TH)-S-.5*RJ))
      BE(I) = AL(I)-PHI-TH
      X(I) = RVAL(I)
      AJ = AIJ
 400  DO 4 6 J = 1,50
      Y(J)=Y(J-1)+DY
      Y(1)=0.
      U(I,J) = SQRT((3.*AJ*SIG)/(4.*RHO*(X(I)+XU)))*(2./(EXP(SIG*Y(J)
     ./(X(I)+XU))+1./EXP(SIG*Y(J)/(X(I)+XU))))**2.
 406  UFLO(I,J) = U(I,J)*(XL+(DEL(I)-Y(J))*COS(BE(I)))
 407  DO 450 J = 1,50
C     NUMERICALLY INTEGRATE VELOCITY DISTRIBUTION TO FIND REATT. LENGTH
      FLOW(I,J) = AREA(UFLO,I,J,DY)
      WRITE(10,410) L(I),Y(J),U(I,J),FLOW(I,J),UFLO(I,J)
 410  FORMAT(5X,F5.4,F10.5,F14.6,F10.5,F15.6)
      IF((FLOW(I,J)-EXFL).GT.0.) GO TO 500
 450  CONTINUE
 500  DELT(I) = Y(J)
      WRITE (10,520) X(I), DELT(I)
 520  FORMAT(5X,F5.4,5X,F10.5)
 540  IF(DELT(I)-DEL(I)) 545,550,55
 545  CONTINUE
 550  CONTINUE
      END
```

A-1

```
                    FUNCTION AREA(Z,I,J,DY)
                    MASS FLOW INTEGRATION BY TRAPEZOIDAL RULE
                    DIMENSION Z(33,50)
                    SUMZ = 0.
5                   N=J-1
                    IF(J.LE..2) GO TO 75
                    DO 70  K = 2,N
70                  SUMZ = SUMZ + Z(I,K)
75                  CONTINUE
10                  AREA = DY/2.*(Z(I,2) + 2.*SUMZ + Z(I,J))
                    IF(J.EQ.1) AREA=0.
                    RETURN
                    END
```

SYMBOLIC REFERENCE MAP (R=1)

ENTRY POINTS
    4 AREA

VARIABLES	SN	TYPE	RELOCATION					
	AREA	REAL				DY	REAL	
	I	INTEGER	F.P.			J	INTEGER	
45	K	INTEGER				N	INTEGER	
43	SUMZ	REAL				Z	REAL	

STATEMENT LABELS
        70   75

LOOPS	LABEL	INDEX	FROM-TO	LENGTH	PROPERTIES
2?	70	K	7 5	33	OPT

STATISTICS
    PROGRAM LENGTH   453
    L(I) STORES OR USED

XFLO = .04355	Y(J)	U(I,J)	FLOW	DFLO(I,J)	
.0100	0.0000 0	177.383134	0.000000	7..48300	
.0100	.000017	177.354403	.000122	7..449.8	
.0100	.000034	177.260317	.000074	7..34.39	
.0100	.000051	177.124471	.000356	7.13. 93	
.0100	.000068	176.924544	.000438	7.12.745	
.0100	.000086	176.657295	.000610	7.1081 0	
.0100	.000103	176.353550	.000731	7..932 5	
.0100	.000127	175.933731	.000552	7..76 50	
.0100	.000137	175.558243	.000073	7. 5568.	
.0100	.000154	175.077745	.001.44	7.035. 5	
.0100	.000171	174.542821	.001224	7.7113.4	
.0100	.000188	173.954174	.001334	6.965456	
.0100	.000205	173.312299	.001453	5.9974 5	
.0100	.000222	172.618270	.001571	5.927394	
.0100	.000239	171.972633	.00001	5.0452.	
.0100	.000257	171.071545	.002017	5.061 62	
.0100	.000274	170.231741	.001949	5.92.73.	
.0100	.000291	161.33002	.002341	5.765 4.	
.0100	.000308	164.34.510	.002126	5.747 58	
.0100	.000325	167.409545	.002271	5.705346	A-2
.0100	.000342	164.377233	.002330	5.66.347	
.0100	.000359	165.364242	.002414	5.610604	
.0100	.000376	160.40238	.002912	5.2697.7	

A-3

.0300	0.000300	99.721239	0.000350	5.345862
.0300	.000017	99.719511	.000071	5.344324
.0300	.000034	99.714725	.000093	5.342614
.0300	.000052	99.705535	.000114	5.340725
		99.690159	.000136	5.338606
		99.666842	.000157	5.336413
.0300		99.632049	.000048	5.334017
.0300	.000121	99.541417	.000039	5.331448
.0300	.000137	99.517194	.000100	5.328650
.0300	.000154	99.789435	.000221	5.325771
.0300	.000171	99.758577	.000012	5.320675
.0300	.000188	99.724452	.000143	5.319477
.0300	.000205	99.687117	.000094	5.315907
.0300	.000222	99.646545	.000185	5.312357
.0300	.000239	99.602753	.000276	5.308576
.0300	.000257	99.555745	.000307	5.304645
.0300	.000274	99.505528	.000457	5.30005
.0300	.000291	99.452108	.000498	5.296205
.0300	.0003 8	99.395492	.001539	5.291757
.0300	.000325	99.335638	.000729	5.287152
.0300	.000342	99.272733	.001017	5.283307
.0300	.000359	99.206545	.001716	5.277376
.0300	.000376	99.137224	.000205	5.272249
.0300	.000393	99.064747	.000207	5.266917
.0300	.000410	98.989124	.002150	5.261499
.0300	.000427	98.910356	.000270	5.255876
.0300	.000445	98.828481	.002100	5.250042
.0300	.000462	98.743451	.002499	5.244202
.0300	.000479	98.655377	.002207	5.238005
.0300	.000496	98.564179	.002029	5.231757
.0300	.000523	98.469399	.002710	5.225302
.0300	.000530	98.372353	.002607	5.218708
.0300	.000547	98.272244	.002696	5.211975
.0300	.000564	98.168693	.002135	5.205103
.0300	.000581	98.062211	.003574	5.197993
.0325	.000593	97.952711	.003253	5.190707
.0300	.000010	97.841203	.003252	5.183304
.0300	.000633	97.724714	.003341	5.175847
.0300	.000650	97.605246	.003429	5.168155
.0300	.000667	97.484317	.003607	5.160301
.0300	.000684	97.352944	.003006	5.152303
.0300	.000702	97.233141	.003914	5.144104
.0300	.000718	97.102925	.003751	5.135505
.0300	.000735	96.969813	.003804	5.127407
.0300	.000752	96.835813	.003857	5.118600
.0300	.000769	96.694953	.004044	5.110276
.0300	.000737	96.553257	.003432	5.101205
.0300	.000804	96.408724	.003404	5.092150
.0300	.000021	96.261331	.004316	5.082907
.0300	.000038	96.111245	.004313	5.073606
.0325	.00 935			
.0400	0.000400	85.343137	0.004000	5.047006
.0400	.000017	85.362445	.004051	5.047052
.0400	.000034	85.363223	.000113	5.047609
.0400	.000051	85.350813	.000022	5.046405
.0400	.000068	85.351332	.000037	5.046479
.0400	.000086	85.344554	.000033	5.045703
.0400	.000103	85.335915	.000047	5.045011
.0400	.000121	85.326347	.000007	5.046021
.0400	.000137	85.315703	.000013	5.046209
.0400	.000154	85.303133	.000730	5.045227
.0400	.000171	85.289123	.000036	5.045989
.0400	.000003	85.273987	.000133	5.043708
.0400	.000003	85.255077	.000044	5.045246
.0400	.000000	85.255474	.000002	5.044060
.0400	.000034	85.310119	.000017	5.046505

A-4

.0400	.000257	85.196677	.001298	5.044..7
.0400	.000274	85.173759	.001334	5.041303
.0400	.000291	85.149393	.001470	5.038623
.0400	.000308	85.123549	.001557	5.035790
.0400	.000325	85.096241	.001643	5. 32884
.0400	.000342	85.067459	.001729	5.029866
.0400	.000359	85.037234	.001815	5.026803
.0400	.000376	85.005541	.001901	5.023654
.0400	.000393	84.972333	.001916	5.020300
.0400	.000410	84.937735	.002072	5.017041
.0400	.000427	84.901727	.002158	5.013818
.0400	.000445	84.864218	.002244	5.010309
.0400	.000462	84.825263	.002329	5.006517
.0400	.000479	84.784862	.002415	5.002841
.0400	.000496	84.743020	.002520	4.99903
.0400	.000513	84.699738	.002506	4.995256
.0400	.000530	84.655020	.002671	4.99139
.0400	.000547	84.608859	.002757	4.987299
.0400	.000564	84.561289	.002842	4.983226
.0400	.000581	84.512280	.002927	4.979050
.0400	.000598	84.461849	.003012	4.974772
.0400	.000616	84.409998	.003097	4.970432
.0400	.000633	84.356733	.003182	4.96609
.0400	.000650	84.302050	.003267	4.961506
.0400	.000667	84.245951	.003352	4.955941
.0400	.000684	84.188465	.003437	4.952255
.0400	.000701	84.129571	.003521	4.947509
.0400	.000718	84.069275	.003506	4.942600
.0400	.000735	84.007592	.003590	4.937715
.0400	.000752	83.944517	.003775	4.932769
.0400	.000769	83.880057	.003559	4.927723
.0400	.000787	83.814217	.003943	4.922578
.0400	.000804	83.747001	.004027	4.917334
.0400	.000821	83.678413	.004111	4.912 52
.0400	.000838	83.608459	.004195	4.906071
.0444		177.383179		

APPENDIX B

Summary of Test Data
Pressure Coefficient Plots

WITHOUT THRUST REVERSER

$P_m = 0$

Pressure Coefficient, C_p

Distance From Nose, inches

$V_{off\ water}/V_t$ — 48, 40, 35

Separation for 40 & 35

B-1

Pressure Coefficient, C_p

$P_n = 30 \text{ psig}$

WITHOUT THRUST REVERSER

Distance From Hose, inches

$V_o = \text{miles/hr}$
48
47
55

B-2

WITH THRUST REVERSER at X = +⅛

$T_m = 0$

Pressure Coefficient, C_p

Distance From Nose, inches

B-3

Pressure Coefficient, C_p

.4 .3 .2 .1 0 -.1 -.2 -.3 -.4 -.5

$P_{in} = 10$ psig

WITH X=+8
THRUST REVERSER

Distance From Nose, inches

B-4

Pressure Coefficient, C_p

$P_{in} = 15\ psig$

WITH eat $X = \frac{L}{8}$

THRUST REVERSER

Distance From Nose, Inches

B-5

Pressure Coefficient, C_p

WITH $X = + \frac{1}{8}$

THRUST REVERSER

$P_{in} = 20$ PSIG

Distance From Nose, Inches

.4 .3 .2 .1 0 -.1 -.2 -.3 -.4 -.5 -.6 -.7 -.8 -.9 -1.0

Pressure Coefficient, C_p

.4 .3 .2 .1 0 -.1 -.2 -.3 -.4 -.5 -.6 -.7 -.8 -.9 -1.0 -1.1 -1.2

Pin=25 psig

WITH THRUST REVERSER $N = +\frac{1}{8}$

Distance From Nose, Inches

Pressure Coefficient, C_p

Distance From Nose, Inches

$P_m = 30$ psig

WITH $x = +\frac{1}{8}$

THRUST REVERSER

B-8

Pressure Coefficient, C_p

WITH $X = + \frac{1}{4}$
THRUST REVERSER
Distance From Nose, Inches

$P_w = 0$

B-9

Pressure Coefficient, C_p

.4 .3 .2 .1 0 -.1 -.2 -.3 -.4

$P_m = 10 \text{ psig}$

WITH
THRUST REVERSER $\quad x = +\frac{1}{4}$

Distance From Nose, inches

B-10

.4 .3 .2 .1 0 -.1 -.2 -.3 -.4

Pressure Coefficient, C_p

.4 .3 .2 .1 0 -.1 -.2 -.3 -.4

$P_{IN} = 15 \, psig$

WITH $X = 4\frac{1}{4}$
THRUST REVERSER

Distance From Nose, inches

B-11

.4 .3 .2 .1 0 -.1 -.2 -.3 -.4

Pressure Coefficient, C_p

WITH $X = + \frac{1}{4}$

THRUST REVERSER

Distance From Nose, inches

$R_n = 200 \text{ psig}$

B-12

Pressure Coefficient, C_p

WITH THRUST REVERSER, $\chi = +\frac{1}{4}$

$P_{in} = 25 psig$

Distance From Nose, inches

B-13

Pressure Coefficient, C_p

Distance From Nose, inches

Run=30psig

WITH
THRUST REVERSER $X=+\frac{1}{4}$

B-14